

Internet Electronic Journal of Molecular Design

April 2003, Volume 2, Number 4, Pages 274–287

Editor: Ovidiu Ivanciuc

Special issue dedicated to Professor Haruo Hosoya on the occasion of the 65th birthday
Part 8

Guest Editor: Jun–ichi Aihara

Three Dimensional Receptor Surface Model of Octopaminergic Agonists for the Locust Neuronal Octopamine Receptor

Akinori Hirashima,¹ Eiichi Kuwano,¹ and Morifusa Eto²

¹ Department of Applied Genetics and Pest Management, Faculty of Agriculture, Graduate School,
Kyushu University, Fukuoka 812–8581, Japan

² Professor Emeritus of Kyushu University, 7–32–2 Aoba, Higashi–ku, Fukuoka 813–0025, Japan

Received: February 13, 2003; Revised: March 28, 2003; Accepted: April 5, 2003; Published: April 30, 2003

Citation of the article:

A. Hirashima, E. Kuwano, and M. Eto, Three Dimensional Receptor Surface Model of Octopaminergic Agonists for the Locust Neuronal Octopamine Receptor, *Internet Electron. J. Mol. Des.* **2003**, 2, 274–287, <http://www.biochempress.com>.

Three Dimensional Receptor Surface Model of Octopaminergic Agonists for the Locust Neuronal Octopamine Receptor[#]

Akinori Hirashima,^{1,*} Eiichi Kuwano,¹ and Morifusa Eto²

¹ Department of Applied Genetics and Pest Management, Faculty of Agriculture, Graduate School,
Kyushu University, Fukuoka 812–8581, Japan

² Professor Emeritus of Kyushu University, 7–32–2 Aoba, Higashi-ku, Fukuoka 813–0025, Japan

Received: February 13, 2003; Revised: March 28, 2003; Accepted: April 5, 2003; Published: April 30, 2003

Internet Electron. J. Mol. Des. 2003, 2 (4), 274–287

Abstract

Motivation. In drug discovery, it is common to have measured activity data for a set of compounds acting upon a particular protein but not to have knowledge of the three-dimensional structure of the protein active site. In the absence of such three-dimensional information, one can attempt to build a hypothetical model of the receptor site that can provide insight about receptor site characteristics. Such a model is known as a receptor surface model (RSM), which provides compact and quantitative descriptors that capture three-dimensional information about a putative receptor site.

Method. All computational experiments were conducted with Cerius2 3.8 quantitative structure–activity relationship (QSAR) environment from Accelrys on a Silicon Graphics O2, running under the IRIX 6.5 operating system. Multiple conformations of each molecule were generated using the Boltzmann Jump as a conformational search method.

Results. The QSAR of a set of 60 octopamine (OA) agonists against receptor 3 in locust nervous tissue was analyzed using RSM. Three-dimensional energetic descriptors were calculated from RSM/ligand interaction and these three-dimensional descriptors were used in the QSAR analysis. The predictive character of the QSAR was further assessed using 10 OA agonists as test molecules.

Conclusions. An RSM was generated using some subset of the most active structures and the results provided useful information in the characterization and differentiation of the OA receptor.

Keywords. *Locusta migratoria*; quantitative structure–activity relationships; QSAR; receptor surface model; Cerius2; octopamine agonist.

Abbreviations and notations

AAT, 2-(aralkylamino)–2-thiazoline	MCSG, maximum common subgroup
AEA, arylethanolamine	mOA, <i>m</i> -hydroxy octopamine
AII, 2-(arylimino)imidazolidine	OA, octopamine
AMT, 2-(aralkylmercapto)–2-thiazoline	PLS, partial least squares
CAII, 2-(2,4,6-trichlorophenylimino)imidazolidine	PRESS, predicted sum of squares
CDM, chlordimeform	RSM, receptor surface model
DMCDM, demethylchlordimeform	SPIT, 3-(substituted phenyl)imidazolidine–2-thione
GFA, genetic function approximation	TMS, tetramethyl silane

[#] Dedicated to Professor Haruo Hosoya on the occasion of the 65th birthday.

* Correspondence author; phone: +81–92–642–2856; fax: +81–92–642–2858; E-mail: ahrasim@agr.kyushu-u.ac.jp.

1 INTRODUCTION

Octopamine [OA, 2-amino-1-(4-hydroxyphenyl)ethanol] which has been found to be present in high concentrations in various insect tissues, is the monohydroxylic analogue of the vertebrate hormone noradrenaline. OA was discovered in the salivary glands of octopus by Erspamer and Boretti in 1951 [1]. It has been found that OA is present in a high concentration in various invertebrate tissues [2]. This multifunctional and naturally occurring biogenic amine has been well studied and established as (1) a neurotransmitter, controlling the firefly light organ and endocrine gland activity in other insects; (2) a neurohormone, inducing mobilization of lipids and carbohydrates; (3) a neuromodulator, acting peripherally on different muscles, fat body, corpora cardiaca, and the corpora allata, and (4) a centrally acting neuromodulator, influencing motor patterns, habituation, and even memory in various invertebrate species [3,4]. The action of OA is mediated through various receptor classes and three different receptor classes OAR1, OAR2A, and OAR2B had been distinguished from non-neuronal tissues [5], in which OAR2 is coupled to G-proteins and is specifically linked to an adenylate cyclase. Thus, the physiological actions of OAR2 were been shown to be associated with elevated levels of cAMP [6]. In the nervous system of locust *Locusta migratoria* L., a particular receptor class was characterized and established as a new class OAR3 by pharmacological investigations of the [³H]OA binding site using various agonists and antagonists [7–11].

Recently much attention has been directed at the octopaminergic system as a valid target in the development of safer and selective pesticides [12–14]. Structure–activity studies of various types of OA agonists and antagonists were also reported using the nervous tissue of the migratory locust, *L. migratoria* L. [7–11]. However, information on the structural requirements of these OA agonists and antagonists for high OA–receptor ligands is still limited. It is therefore of critical importance to provide information on the pharmacological properties of this OA–receptor types and subtypes. Our interest in OA agonists was stimulated by the results of quantitative structure–activity relationship (QSAR) studies using various physico–chemical parameters as descriptors [15,16] and receptor surface model (RSM) [17]. Furthermore, molecular modeling and conformational analysis were performed in Catalyst/Hypo to gain a better knowledge of the interactions between OA antagonists and OAR3 in order to understand the conformations required for binding activity [18]. A similar procedure was repeated using OA agonists [19]. In drug discovery, it is common to have measured activity data for a set of compounds acting upon a particular protein but not to have knowledge of the three–dimensional structure of the protein active site. In the absence of such three–dimensional information, one can attempt to build a hypothetical model of the receptor site that can provide insight about receptor site characteristics. Such a model is known as an RSM, which provides compact and quantitative descriptors that capture three–dimensional information about a putative receptor site. Thus, the current work is aimed to perform 3D RSM on a set of OA agonists against OAR3 in thoracic nerve system of *L. migratoria*.

2 MATERIALS AND METHODS

2.1 Synthesis of OA agonists

2-(Aralkylamino)-2-thiazolines (AATs) **1–26** and **61–64** were synthesized by cyclization of the corresponding thiourea with conc. hydrogen chloride [20]. 3-(Substituted phenyl)imidazolidine-2-thiones (SPITs) **42–44** and **66–68** were synthesized by the cyclization of monoethanolamine hydrogen sulfate with the corresponding arylisothiocyanate in the presence of sodium hydroxide as described in the previous report [21].

2-(Aralkylmercapto)-2-thiazolines (AMTs) **48–49** were obtained by stirring 2-mercaptothiazoline and the corresponding aralkyl halogen overnight in pyridine [20]. The structures of the compounds were confirmed by ^1H -, ^{13}C -NMR measured with a JEOL JNM-EX400 spectrometer at 400 MHz, tetramethyl silane (TMS) being used as an internal standard for ^1H NMR, and elemental analytical data. Data for other compounds 2-(arylimino)imidazolidine (AII) **27–41**, aryloethanolamine (AEA) **45–47**, **50–53**, chlordimeform (CDM) **54**, **55–60**, 2-(2,4,6-trichlorophenylimino)imidazolidine (CAII) **65**, *m*-hydroxy octopamine (mOA) **69**, and demethylchlordimeform (DMCDM) **70** was cited from Ref. [10].

2.2 Computational Details

2.2.1 Molecular alignment

All computational experiments were conducted with Cerius2 3.8 QSAR environment from Accelrys (San Diego, USA) on a Silicon Graphics O2, running under the IRIX 6.5 operating system. Multiple conformations of each molecule were generated using the Boltzmann Jump as a conformational search method. The upper limit of the number of conformations per molecule was 150. Each conformer was subjected to an energy minimization procedure to generate the lowest energy conformation for each structure.

Alignment of structures through pair-wise superposition placed all structures in the study compounds in the same frame of reference as the shape reference compound, which was selected as a conformer of the most active OA agonist. The method used for performing the alignment was maximum common subgroup (MCSG). This method looks at molecules as points and lines, and uses the techniques of graph theory to identify patterns. It finds the largest subset of atoms in the shape reference compound that is shared by all the structures in the study table and uses this subset for alignment. A rigid fit of atom pairings was performed to superimpose each structure so that it overlays the shape reference compound.

2.2.2 Receptor surface model

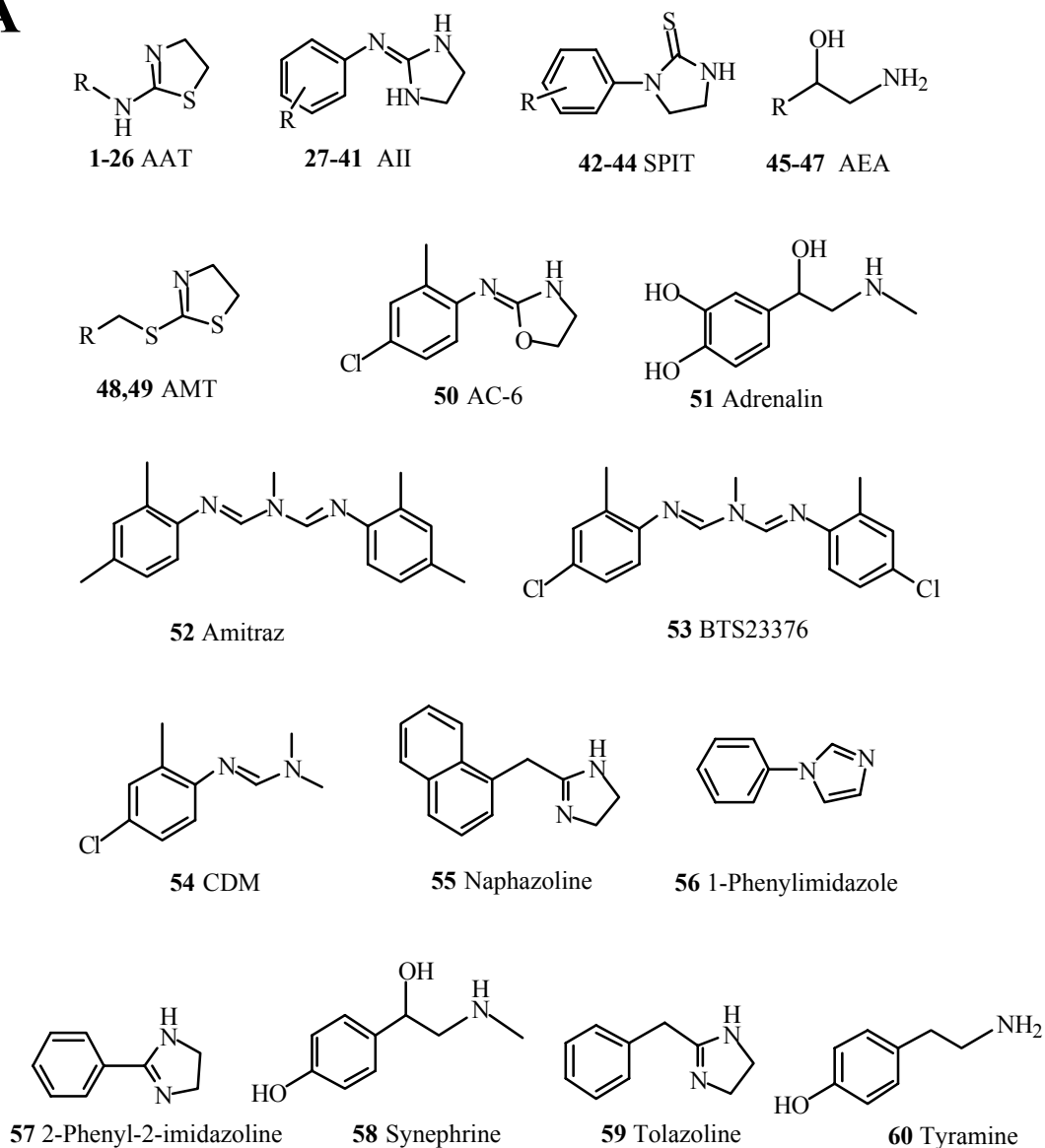
RSM models proposed by Hahn [22,23] are predictive and sufficiently reliable to guide the chemist in the design of novel compounds. These descriptors are used for predictive QSAR models. This approach is effective for the analysis of data sets where activity information is available but the structure of the receptor site is unknown. Thus, activity data was used for generating the RSM. RSM attempts to postulate and represent the essential features of a receptor site from the aligned common features of the molecules that bind to it. This method generates multiple models that can be checked easily for validity. The RSM model was tested for prediction with the leave-one-out cross-validation method. Once a reasonable RSM has been defined, a series of structures can be evaluated against the model. When a receptor model has been generated and the models have been aligned, a QSAR can be built using data from the receptor-structure interactions. The results of the minimization procedure were used as descriptors either to refine the model or to predict activity. For prediction, the molecules were minimized in the RSA receptor. Three-dimensional energetic descriptors were calculated from RSM/ligand interaction. These three-dimensional descriptors were used in the QSAR analysis.

An RSM represents the global volume that can accommodate one or more molecules and can be seen as the shape of an active site built from the ligands that fit into it in their “active” conformation. The descriptors used in this study account for phenomena that occur at the contact surface between the ligands and the protein active site. An RSM represents essential information about the hypothetical receptor site as a three-dimensional surface with associated properties mapped onto the surface model. The location and shape of the surface represent information about the steric nature of the receptor site: the associated properties represent other information of interest, such as hydrophobicity, partial charge, electrostatic potential, and hydrogen-bonding propensity. The isosurface procedure produces a surface that entirely encloses the molecules over which it is generated. The surface has no holes and is known as a closed model. RSMs are best constructed from a set of the most active analogues that are chosen to cover the variety of steric and electrostatic variations likely to appear in the test data. The approach we took was to automatically build a set of different RSMs from different combinations of the most active analogues, and then use a variable-selection technique such as genetic partial least squares (G/PLS) to discover the RSM whose descriptors yield the best QSARs of the full training set. G/PLS allows the discovery and use of nonlinear descriptors by using spline-based terms.

2.2.3 G/PLS

G/PLS, a variation of genetic function approximation (GFA), was run as an alternative to the standard GFA algorithm. G/PLS is derived from the best features of two methods: GFA and partial least squares (PLS). Both GFA and PLS have been shown to be valuable analysis tools in cases where the data set has more descriptors than samples.

A



B

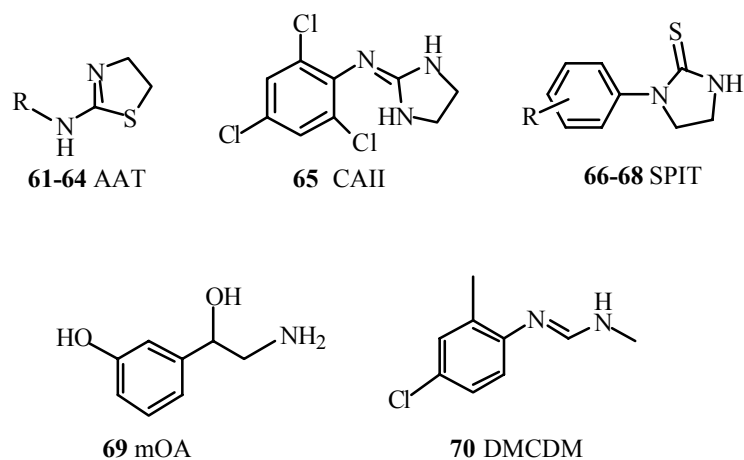


Figure 1. Structures of OA agonists used for regression analysis in study (A) and test (B) sets.

In PLS, variables might be overlooked during interpretation or in designing the next experiment even though cumulatively they are very important. This phenomenon is known as “loading spread”. In GFA, equation models have a randomly chosen proper subset of the independent variables. As a result of multiple linear regression on each model, the best ones become the next generation and two of them produce an offspring. This was repeated 10000 (default 5000) times. For other settings, all defaults were used. Loading spread does not occur because at most one of a set of co-linear variables is retained in each model. G/PLS combines the best features of GFA and PLS (Cerius2 tutorial, Accelrys Inc., <http://www.accelrys.com/cerius2>) and actually G/PLS gave better results than in cases when GFA or PLS was used. G/PLS retains the ease of interpretation of GFA by back-transforming the PLS components to the original variables.

Table 1. Regression Analysis of Structure–OA Agonist Activities in the Study Set

No	Compound R	K _i (nM)	pK _i		
			Observed	Calculated ^a	Deviation
AAT					
1	PhCH ₂	280±59 ^b	6.55	7.03	-0.48
2	2-Cl-PhCH ₂	440±189 ^b	6.36	6.74	-0.38
3	2-F-PhCH ₂	447±125 ^b	6.35	6.76	-0.41
4	2-CH ₃ -PhCH ₂	650±360 ^b	6.19	5.79	0.40
5	2-CF ₃ -PhCH ₂	290±203 ^b	6.54	6.21	0.33
6	3-Cl-PhCH ₂	95±66 ^b	7.02	6.73	0.29
7	3-F-PhCH ₂	250±75 ^b	6.60	6.66	-0.06
8	3-CH ₃ -PhCH ₂	34±26 ^b	7.47	6.68	0.79
9	3-CF ₃ -PhCH ₂	380±266 ^b	6.42	6.75	-0.33
10	3-NO ₂ -PhCH ₂	185±33 ^b	6.73	6.67	0.06
11	4-Cl-PhCH ₂	89±6 ^b	7.05	6.66	0.39
12	4-F-PhCH ₂	460±124 ^b	6.34	6.66	-0.32
13	4-CH ₃ -PhCH ₂	38±16 ^b	7.42	6.89	0.53
14	2,3-Cl ₂ -PhCH ₂	42±19 ^b	7.38	6.83	0.55
15	2-Cl,4-F-PhCH ₂	184±90 ^b	6.74	7.22	-0.48
16	2,5-Cl ₂ -PhCH ₂	132±83 ^b	6.88	6.33	0.55
17	2,6-Cl ₂ -PhCH ₂	1270±635 ^b	5.90	6.35	-0.45
18	3-Cl,4-F-PhCH ₂	109±59 ^b	6.96	6.66	0.30
19	3,4-F ₂ -PhCH ₂	445±196 ^b	6.35	6.66	-0.31
20	PhCH ₂ CH(L)	37±23 ^b	7.43	7.91	-0.48
21	PhCH ₂ CH(D)	5000±2600 ^b	5.30	5.86	-0.56
22	PhCH ₂ CH ₂	5500±1920 ^b	5.26	5.46	-0.20
23	4-Cl-PhCH ₂ CH ₂	264±95 ^b	6.58	6.39	0.19
24	3-PyridylCH ₂	8330±2500 ^b	5.08	4.83	0.25
25	1-Morpholino(CH ₂) ₂	70800±19000 ^b	4.15	4.28	-0.13
26	1-Morpholino(CH ₂) ₃	121000±31400 ^b	3.92	4.12	-0.20
All					
27	H	23±5 ^c	7.63	7.63	0
28	4-Br	15±3 ^c	7.83	7.59	0.24
29	2,4-Cl ₂	0.81±0.18 ^c	9.09	8.99	0.10
30	2-CH ₃ ,4-Cl	0.87±0.32 ^c	9.06	8.91	0.15
31	2,4-(CH ₃) ₂	1.02±0.42 ^c	8.99	8.90	0.09
32	2,6-Cl ₂	47±18 ^c	7.32	7.45	-0.13
33	2,6-(CH ₃) ₂	20±7 ^c	7.70	7.62	0.08
34	2,6-(CH ₂ CH ₃) ₂	0.3±0.04 ^c	9.54	8.92	0.62
35	2,6-[CH(CH ₃) ₂] ₂	132±35.6 ^c	6.88	7.72	-0.84

Table 1. (Continued).

No	Compound R	Ki (nM)	pKi		
			Observed	Calculated ^a	Deviation
36	2,4,6-Cl ₃	19±3 ^c	7.73	7.98	-0.25
37	2,6-Cl ₂ ,4-NH ₂	58±16 ^c	7.24	7.34	-0.10
38	2,6-Cl ₂ ,4-N ₃	44.5±7.1 ^c	7.35	7.65	-0.30
39	2,4,6-(CH ₃) ₃	4.38±1.30 ^c	8.36	7.92	0.44
40	2,4,6-(CH ₂ CH ₃) ₃	0.56±0.14 ^c	9.25	9.09	0.16
41	2,6-(CH ₂ CH ₃) ₂ ,4-N ₃	1.05±0.47 ^c	8.98	8.99	-0.01
SPIT					
42	4-Cl	280±134 ^b	6.55	6.35	0.20
43	2,6-(CH ₂ CH ₃) ₂	170±51 ^b	6.77	6.76	0.01
44	2,4,5-Cl ₃ -PhCH ₂	1040±730 ^b	5.98	6.41	-0.43
AEA					
45	Ph (DL)	115±39 ^c	6.94	6.80	0.14
46	4-OH-Ph	7.9±0.9 ^c	8.18	8.55	-0.37
47	3,4-(OH) ₂ -Ph	475±42 ^c	6.32	6.80	-0.48
AMT					
48	PhCH ₂	760±243 ^b	6.12	6.81	-0.69
49	4-Cl-PhCO	17500±3670 ^b	4.76	5.19	-0.43
50	AC-6	0.95±0.24 ^c	9.02	8.87	0.15
51	Adrenalin	416±75 ^c	6.38	7.43	-1.05
52	Amitraz	22±5 ^c	7.67	7.29	0.38
53	BTS23376	8.9±0.6 ^c	8.05	8.33	-0.28
54	CDM	137±70 ^c	6.91	7.14	-0.23
55	Naphazoline	3.03±2.61 ^c	8.52	7.85	0.67
56	Phenylimidazole	813±561 ^c	6.09	6.64	-0.55
57	2-Phenyl-2-imidazolidine	16200±4700 ^c	4.79	3.99	0.80
58	Syneprine	3.38±0.64 ^c	8.47	7.76	0.71
59	Tolazoline	18.5±16 ^c	7.73	6.91	0.82
60	Tyramine	51.6±17.5 ^c	7.29	6.77	0.52

^a Calculated by Eq. (1)

^b Personal communication (T. Roeder, Hamburg University, Germany)

^c Cited from Ref. [10]

Table 2. Regression Analysis of Structure-OA Activities in Test Set

No	Compound R	Ki (nM)	pKi		
			Observed	Calculated ^a	Deviation
AAT					
61	4-OCH ₃ -PhCH ₂	9.0±6.3 ^b	8.05	5.83	2.22
62	2,4-Cl ₂ -PhCH ₂	1.7±1.1 ^b	8.77	9.29	-0.52
63	3,4-Cl ₂ -PhCH ₂	14.0±4.2 ^b	7.85	6.93	0.92
64	3,5-Cl ₂ -PhCH ₂	1 ^b	9.00	6.13	2.87
65	CAII	2.27±0.89 ^c	8.64	8.49	0.15
SPIT					
66	2,3-Cl ₂	37100±7770 ^b	4.43	6.36	-1.93
67	2-CH ₃ ,4-Cl	20±9 ^b	7.70	6.45	1.25
68	2,4-(CH ₃) ₂	1660±700 ^b	5.78	6.44	-0.66
69	mOA	5050±1860 ^c	5.30	6.66	-1.36
70	DMCDM	1.97±0.76 ^c	8.74	7.23	1.51

^a Calculated by Eq. (1)

^b Personal communication (T. Roeder, Hamburg University, Germany)

^c Cited from Ref. [10]

3 RESULTS AND DISCUSSION

A set of 60 molecules, whose inhibitory activities were tested elsewhere using the [^3H]-OA binding to OAR3 in the locust central nervous tissue, was selected from published data [10] or obtained by personal communication (T. Roeder, Hamburg University, Germany) as the target training set. The molecular structures and experimental biological activities are listed in Figure 1a and Table 1. Some models were statistically significant and were used to correctly predict the activities of a set of test molecules ranging over 5 orders of magnitude (max. pK_i 9.54 and min. pK_i 3.92), indicating that these models could be useful tools to design active OA agonists. This method generates multiple models that can be checked easily for validity.

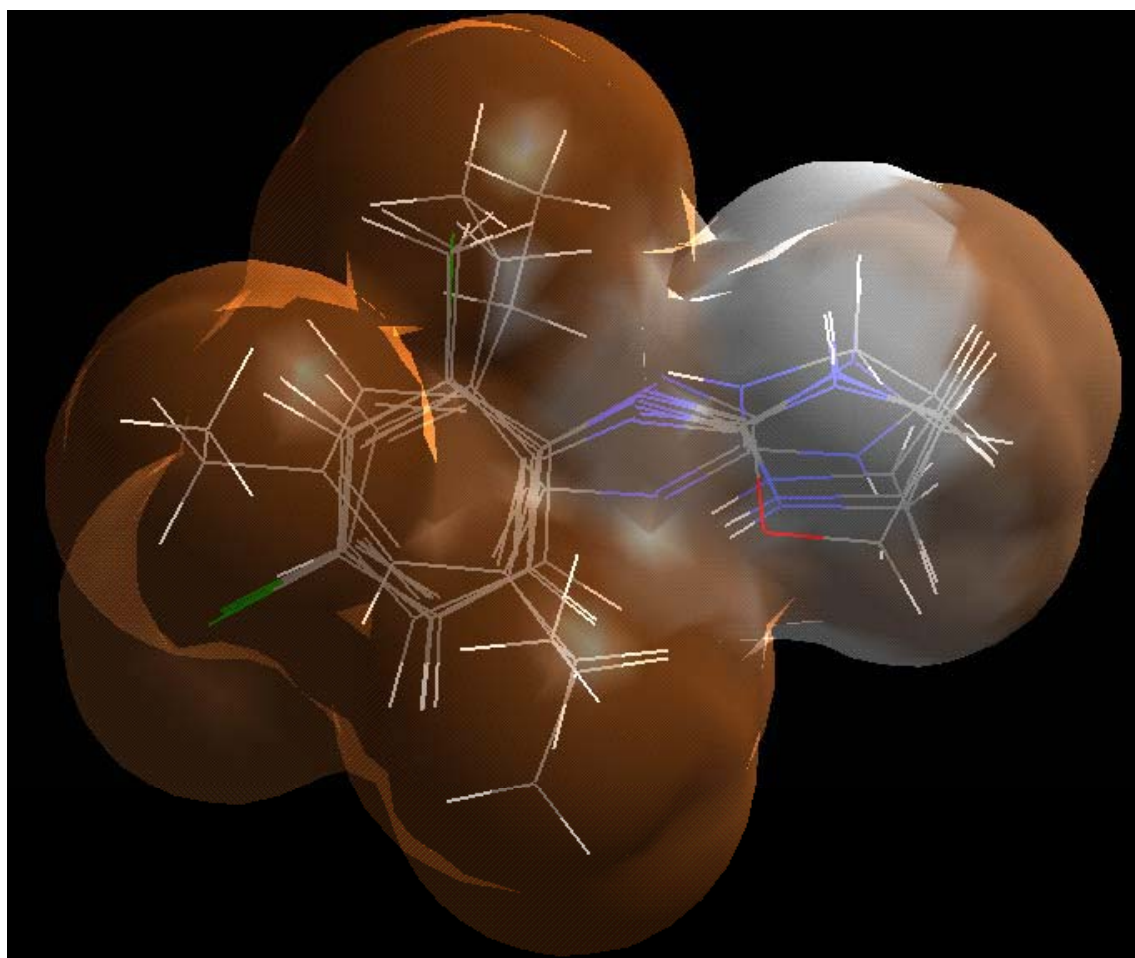


Figure 2. The top OA agonists **29**, **30**, **34**, **40**, and **50** embedded in an RSM generated from them computed with the van der Waals function colored by hydrophobicity: a brown color stands for a positive contribution of hydrophobicity and a gray color stands for a negative contribution of hydrophobicity. The phenyl rings and their substituents are hydrophobic, while the heterorings such as imidazolidine and oxazolidine rings are hydrophilic.

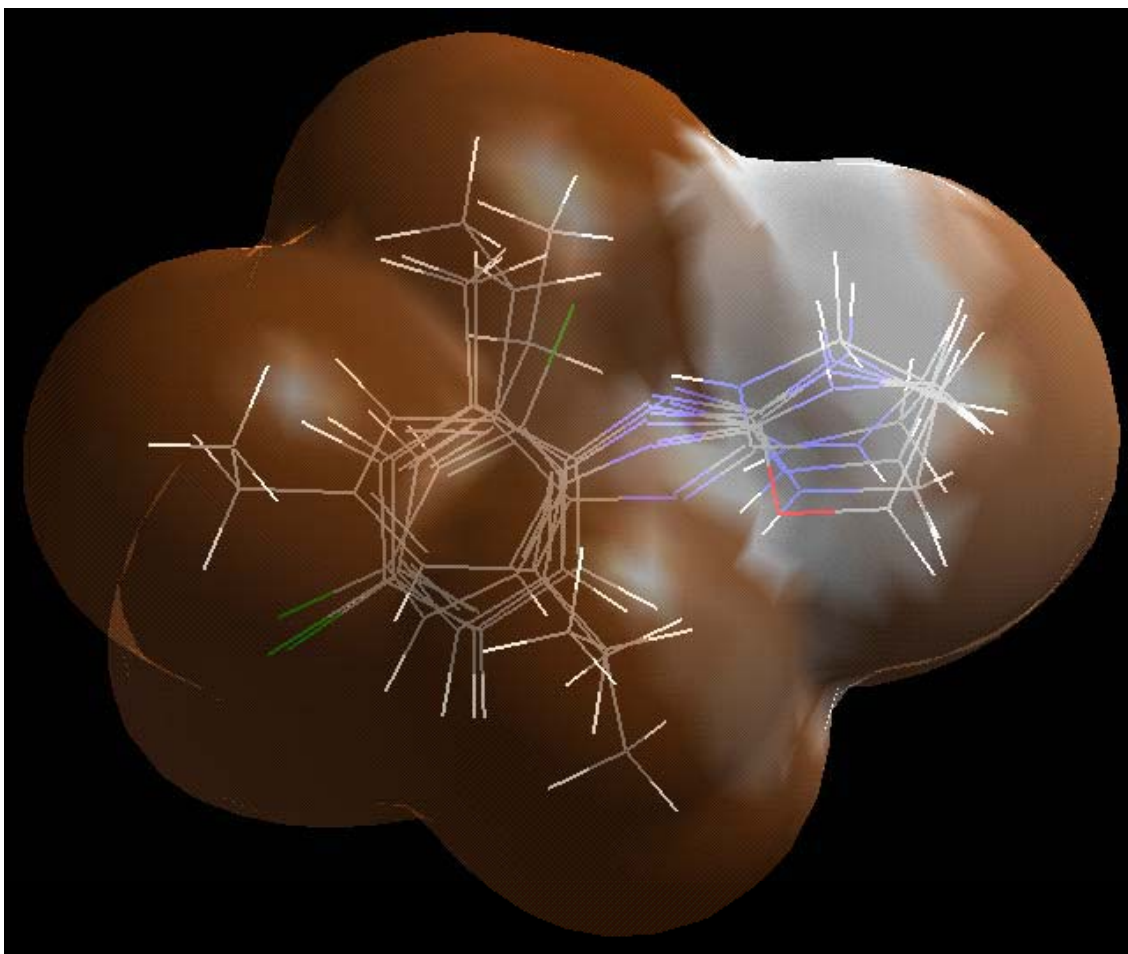


Figure 3. The top OA agonists **29**, **30**, **34**, **40**, and **50** embedded in an RSM generated from them computed with the Wyvill steric function colored by hydrophobicity: a brown color stands for a positive contribution of hydrophobicity and a gray color stands for a negative contribution of hydrophobicity. The phenyl rings and their substituents are hydrophobic, while the heterorings such as imidazolidine and oxazolidine rings are hydrophilic.

2-(2,6-Diethylphenylimino)imidazolidine **34** showed the highest activity followed by **40**, **29**, **30**, and 1-(2-methyl-4-chlorophenyl)oxazolidine **50** in study compounds. An RSM was generated (Figures 2 and 3) using some subset of the most active structures (**29**, **30**, **34**, **40**, and **50**). The rationale underlying this model is that the most active structures tend to explore the best spatial and electronic interactions with receptor, while the least active ones do not and tend to have unfavorable steric or electronic interactions. A rigid fit was performed to superimpose each structure so that it overlays the shape reference compound AII **34**. OA agonists **29**, **30**, **34**, **40**, and **50** were used to generate an RSM with the van der Waals function (Figure 2) or the Wyvill steric function (Figure 3). The van der Waals steric function gives a hard receptor, very similar with the surface area of the compounds that generate the receptor, while the Wyvill steric function gives a soft receptor, a fuzzy representation of the molecular surface area, with much larger limits. A comparison between the shapes of the van der Waals and Wyvill receptors from Figures 2 and 3 clearly shows the differences between them: while in the former the shape of the atoms can be easily recognized, the

later has a fuzzy shape, with a larger distance between atoms and the surface points. The RSM is colored by hydrophobicity: a brown color stands for a positive contribution of hydrophobicity and a gray color stands for a negative contribution of hydrophobicity. The brown regions are spread almost on the entire molecule, with the exception of heteroring regions colored in gray: the phenyl rings and their substituents are hydrophobic, while the heterorings such as imidazolidine and oxazolidine rings are hydrophilic. This color coding of the ligand–receptor interactions can offer a qualitative way of examining compounds, by introducing them into the virtual receptor and visually inspecting the favorable/unfavorable interactions; substituents that increase or decrease the binding affinity can be easily recognized, and one can make easily simple but accurate structure–activity estimations.

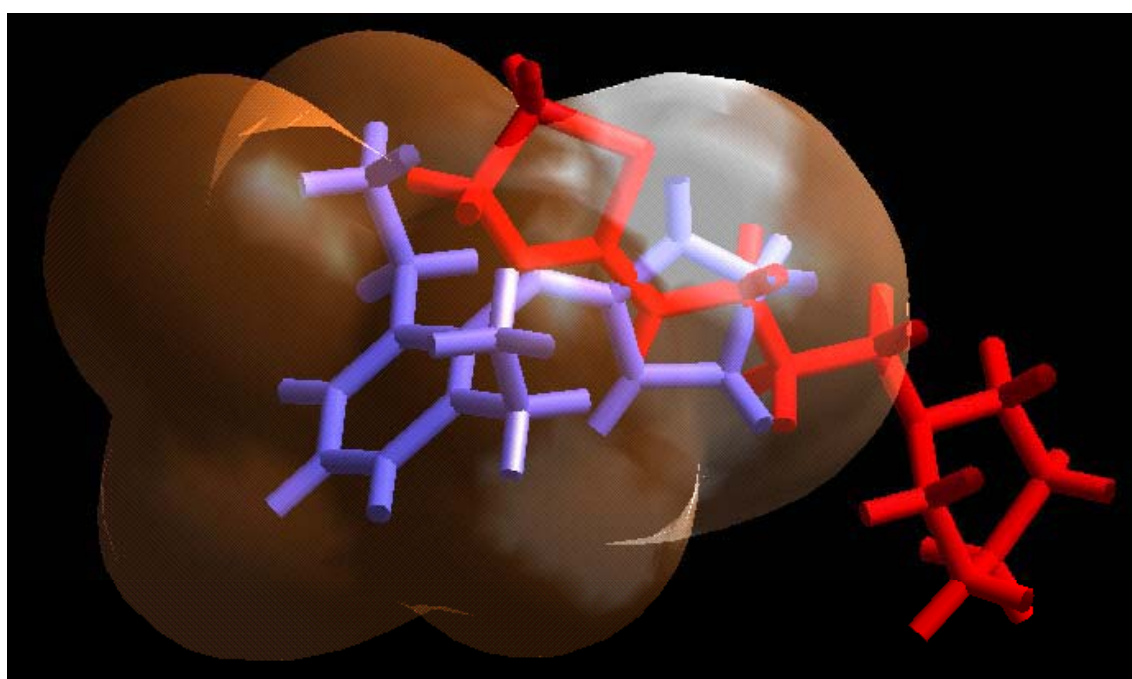


Figure 4. The OA agonists **34** (blue) with the highest activity and **26** (red) with lowest activity embedded in an RSM generated from top 5 compounds computed with the Wyvill steric function colored by hydrophobicity: a brown color stands for a positive contribution of hydrophobicity and a gray color stands for a negative contribution of hydrophobicity. The RSM is embedded with the most active OA agonist **34**, while the morpholine ring and the part of thiazolidine ring of the least active OA agonist **26** stick out of the RSM and thus **26** is in an undesirable position.

Figure 4 shows the OA agonist AII **34** with the highest activity and the OA agonist 1–morpholino(CH₂)₃ AAT **26** with the lowest activity embedded in an RSM generated from the top 5 molecules. The RSM is embedded with the most active OA agonist **34**, while the morpholine ring and the part of thiazolidine ring of the least active OA agonist **26** stick out of the RSM and thus **26** is in an undesirable position for OA–agonist activity.

The energies of interaction between the RSM and each molecular model were added to the study table as new columns, which were used for generating QSARs. Instead of one total number that is

the sum of the interactions evaluated between each point on the surface and each molecular model, leading to one extra column in the study table, the energies at each surface point are available. Depending on the size of the drug molecules, this is potentially a great number of surface points. In order to quantitatively understand the dependence of biological activities on RSM parameters of OA agonists, regression analysis was applied to representative 60 study compounds listed in Figure 1a and Table 1. The best model generated using the descriptors from the closed RSM is given in Eq. (1), which is similar with the 4D QSAR of Hong and Hopfinger [24]. The number of variables for Eq. (1) was 1730. Ten percent of all new significant columns of variables were automatically used as independent X variables in the generation of QSAR.

$$\begin{aligned}
 pKi = & 4.6889 + 3.30753VDW/923 + 3.31227(VDW/1399)^2 - 5.83577(VDW/1573)^2 \\
 & - 3.64963(VDW/3186)^2 + 7.75413(VDW/3378 + 0.253053) - 2.45429(VDW/4243 \\
 & + 0.13452) + 4.84734(TOT/1768 + 0.348396) + 5.04467(TOT/2438 - 0.004453)^2 \\
 & + 5.01541(TOT/2438 + 0.003512)^2 - 1.4234TOT/3751 + 4.45962(TOT/4301 \\
 & + 0.014739)^2 + 4.47306(TOT/4301 + 0.013958)^2 + 6.14155(TOT/4377)^2 \\
 & - 6.80091(TOT/4687)^2
 \end{aligned} \tag{1}$$

where $n = 60$, $r^2 = 0.877$, $CV-r^2 = 0.766$, $PRESS = 21.208$, and $Bsr^2 = 0.871 \pm 0.026$. The descriptors $VDW/923$, $VDW/1399$, etc are the Van der Waals interaction energy of the molecule with the receptor at point 923, 1399, etc. The descriptors $TOT/1768$, $TOT/2438$, etc are added energy of both electrostatic interaction energy and Van der Waals interaction energy at point 1769, 2438, etc. The term n means the number of data points; r -squared (r^2), the square of the correlation coefficient, which is used to describe the goodness of fit of the data of the study compounds to the QSAR model; cross-validated r^2 ($CV-r^2$), a squared correlation coefficient generated during a validation procedure using the equation: $CV-r^2 = (SD - PRESS)/SD$; predicted sum of squares (PRESS), the sum of overall compounds of the squared differences between the actual and the predicted values for the dependent variables; SD, the sum of squared deviations of the dependent variable values from their mean. The PRESS value is computed during a validation procedure for the entire training set. The larger the PRESS value, the more reliable is the equation. A $CV-r^2$ is usually smaller than the overall r^2 for a QSAR equation. It is used as a diagnostic tool to evaluate the predictive power of an equation generated using the G/PLS method. Cross-validation is often used to determine how large a model (number of terms) can be used for a given data set. For instance, the number of components retained in G/PLS can be selected to be that which gives the highest $CV-r^2$. Bootstrap r^2 (Bsr^2) is the average squared correlation coefficient calculated during the validation procedure (Cerius2 tutorial, Accelrys Inc., <http://www.accelrys.com/cerius2>). A Bsr^2 is computed from the subset of variables used one-at-a-time for the validation procedure. It can be used more than one time in computing the r^2 statistic. Table 1 depicts structures of OA agonists, their experimental K_i values, calculated pKi values using Eq. (1), and difference between observed and calculated pKi values. In case predicted activity is overestimated, deviation is obtained by calculating predicted activity subtracted by experimental value and indicated by minus. In case predicted activity is

underestimated, deviation is obtained by calculating experimental activity subtracted by predicted value. The RSM was statistically significant and used to correctly predict the activities of a set of training molecules, indicating that these models could be useful tools to design active OA agonists.

Once the desired RSM has been constructed, all the structures in the test sets were evaluated against the model. The evaluation consists of computing several energetic descriptors that are based upon the interactions between ligand and model. By using receptor data to develop a QSAR model, the goodness of fit can be evaluated between a candidate structure and a postulated pseudo-receptor. The predictive character of the QSAR was further assessed using 10 OA agonists as test molecules, whose structures are shown in Figure 1b, outside of the training set. The best statistically significant Eq. (1) was applied to access these OA agonists. The predicted values of these molecules are listed in Table 2, which depicts OA agonists, their experimental K_i values, calculated pK_i values using Eq. (1), and difference between observed and calculated pK_i values. Some OA agonists were active according to Eq. (1) in inhibiting the binding of [^3H]OA to OAR3. A distinguishing characteristic of the Eq. (1) is that it has a strong tendency to underestimate the OA-agonist activity especially of **61**, **64**, and **70** (experimental pK_i : 8.05, 9.00, and 8.74; estimated pK_i : 5.83, 6.13, and 7.23, respectively). Meanwhile, it overestimated slightly the OA-agonist activity of **66** and **69** (experimental pK_i : 4.43 and 5.30; estimated pK_i : 6.36 and 6.66, respectively). Although the process of evaluating the RSM for OA agonists does not treat these OA agonists reasonably, the activity of OA agonists **62**, **63**, **65**, and **68** were predicted reasonably.

4 CONCLUSIONS

RSMs are quantitative QSAR and differ from pharmacophore models, which are qualitative, in that the former tries to capture essential information about the receptor, while the latter only captures information about the commonality of compounds that bind. RSMs tend to be geometrically overconstrained (and topologically neutral) since, in the absence of steric variation in a region, they assume the tightest steric surface that fits all training compounds. RSMs do not contain atoms, but try to directly represent the essential features of an active site by assuming complementarity between the shape and properties of the receptor site and the set of binding compounds. The RSM application uses 3D surfaces that define the shape of the receptor site by enclosing the most active members (after appropriate alignment) of a series of compounds. The global minimum of the most active compound **34** in the study compounds (based on the value in the activity column) was made as the active conformer. It really is just one of possibly many self-consistent models that fit the biological activity data. This model ought to be predictive and sufficiently reliable to guide the chemist in the design of novel compounds. These descriptors were used for predictive QSAR models. This approach is effective for the analysis of data sets where activity information is available but the structure of the receptor site is unknown. RSM attempts to

postulate and represent the essential features of a receptor site itself, rather than the common features of the molecules that bind to it.

OA is not likely to penetrate either the cuticle or the central nervous system of insects effectively, since it is fully ionized at physiological pH. Derivatization of the polar groups would be one possible solution to this problem in trying to develop potential pest-control agents. The above RSM studies show that agonists with 2,6-diethyl substituents can be potential ligands to OA receptors. However, phenyl ring substitution requirements for OA agonists differ substantially from each other and other various types of OA agonists could be potent, although the type of compounds tested here is still limited to draw any conclusions. These derivatives could provide useful information in the characterization and differentiation of OA receptor. They may help to point the way towards developing extremely potent and relatively specific OA ligands, leading to potential insecticides, such as inhibitors of sex-pheromone production [25], although further research on the comparison of the 3D QSAR from OA agonists is necessary. In order to optimize the activities of these compounds as OA ligands, more detailed experiments are in progress. Additionally, binding activity is not enough for evaluating OA-agonist activity, since in binding assay it is difficult to say the difference of activities between OA agonists and antagonists. Thus, the work is going to be published elsewhere to perform 3D RSM on a set of OA agonists against thoracic nerve system of American cockroach *Periplaneta americana*, in which OA-agonist action is supposed to be due to cAMP elevation at OAR2 [13].

Acknowledgment

This work was supported in part by a Grant-in-Aid for Scientific Research from the Ministry of Education, Science, and Culture of Japan.

5 REFERENCES

- [1] V. Erspamer and G. Boretti, Identification and characterization by paper chromatography of enteramine, octopamine, tyramine, histamine, and allied substances in extracts of posterior salivary glands of Octopoda and in other tissues of vertebrates and invertebrates, *Arch. Int. Pharmacodyn.* **1951**, 88, 296–332.
- [2] J. Axelrod and J. M. Saavedra, Octopamine, *Nature* **1977**, 265, 501–504.
- [3] P. D. Evans, Molecular studies on insect octopamine receptors; in: *Comparative Molecular Neurobiology*, Ed. S. R. Heller, Birkhäuser Verlag, Basel, 1993, pp. 286–296.
- [4] P. D. Evans, Octopamine; in: *Comprehensive Insect Physiology Biochemistry Pharmacology*, Eds. G. A. Kerkut and G. Gilbert, Pergamon Press, Oxford, 1985, Vol 11, pp. 499–530.
- [5] P. D. Evans, Multiple receptor types for octopamine in the locust, *J. Physiol.* **1981**, 318, 99–122.
- [6] J. A. Nathanson, Phenyliminoimidazolidines, Characterization of a class of potent agonists of octopamine-sensitive adenylate cyclase and their use in understanding the pharmacology of octopamine receptors, *Mol. Pharmac.* **1985**, 28, 254–268.
- [7] T. Roeder and J. A. Nathanson, Characterization of insect neuronal octopamine receptors (OA3 receptors), *Neurochem. Res.* **1993**, 18, 921–925.
- [8] T. Roeder and M. Gewecke, Octopamine receptors in locust nervous tissue, *Biochem. Pharm.* **1990**, 39, 1793–1797.
- [9] T. Roeder, A new octopamine receptor class in locust nervous tissue, the octopamine 3 (OA3) receptor, *Life Science* **1992**, 50, 21–28.
- [10] T. Roeder, Pharmacology of the octopamine receptor from locust central nervous tissue (OAR3), *Br. J. Pharmac.*

- 1995**, 114, 210–216.
- [11] T. Roeder, High-affinity antagonists of the locust neuronal octopamine receptor, *Eur. J. Pharmac.* **1990**, 191, 221–224.
- [12] K. R. Jennings, D. G. Kuhn, C. F. Kukel, S. H. Trotto, and W. K. Whitenev, A biorationally synthesized octopaminergic insecticide: 2-(4-chloro-*o*-toluidino)-2-oxazoline, *Pestic. Biochem. Physiol.* **1988**, 30, 190–197.
- [13] A. Hirashima, Y. Yoshii, and M. Eto, Action of 2-aryliminothiazolidines on octopamine-sensitive adenylate cyclase in the American cockroach nerve cord and on the two-spotted spider mite *Tetranychus urticae* Koch, *Pestic. Biochem. Physiol.* **1992**, 44, 101–107.
- [14] S. M. M. Ismail, R. A. Baines, R. G. H. Downer, and M. A. Dekeyser, Dihydrooxadiazines: Octopaminergic system as a potential site of insecticidal action, *Pestic. Sci.* **1996**, 46, 163–170.
- [15] A. Hirashima, K. Shinkai, C. Pan, E. Kuwano, E. Taniguchi, and M. Eto, Quantitative structure-activity studies of octopaminergic ligands against *Locusta migratoria* and *Periplaneta americana*, *Pestic. Sci.* **1999**, 55, 119–128.
- [16] C. Pan, A. Hirashima, J. Tomita, E. Kuwano, E. Taniguchi, and M. Eto, Quantitative structure-activity relationship studies and molecular modelling of octopaminergic 2-(substituted benzylamino)-2-thiazolines and oxazolines against nervous system of *Periplaneta americana* L., *Internet J. Sci.-Biol. Chem.* **1997**, 1, <http://www.netsci-journal.com/97v1/97013/index.htm>.
- [17] A. Hirashima, C. Pan, J. Tomita, E. Kuwano, E. Taniguchi, and M. Eto, Quantitative structure-activity studies of octopaminergic agonists and antagonists against nervous system of *Locusta migratoria*, *Bioorg. Med. Chem.* **1998**, 6, 903–910.
- [18] C. Pan, A. Hirashima, E. Kuwano, and M. Eto, Three-dimensional pharmacophore hypotheses for the locust neuronal octopamine receptor (OAR3): 1. Antagonists, *J. Molec. Model.* **1997**, 3, 455–463.
- [19] A. Hirashima, C. Pan, E. Kuwano, E. Taniguchi, and M. Eto, Three-dimensional pharmacophore hypotheses for the locust neuronal octopamine receptor (OAR3): 2. Agonists, *Bioorg. Med. Chem.* **1999**, 7, 1437–1443.
- [20] A. Hirashima, Y. Yoshii, and M. Eto, Synthesis and octopaminergic agonist activity of 2-(substituted benzylamino)-2-thiazolines, *Biosci. Biotech. Biochem.* **1992**, 56, 1062–1065.
- [21] A. Hirashima, K. Shinkai, E. Kuwano, E. Taniguchi, and M. Eto, Synthesis and octopaminergic-agonist activity of 3-(substituted phenyl)imidazolidine-2-thiones and related compounds, *Biosci. Biotech. Biochem.* **1998**, 62, 1179–1184.
- [22] M. Hahn, Receptor surface models. 1. Definition and construction, *J. Med. Chem.* **1995**, 38, 2080–2090.
- [23] M. Hahn and D. Rogers, Receptor surface models. 2. Application to quantitative structure-activity-relationships studies, *J. Med. Chem.* **1995**, 38, 2091–2102.
- [24] X. Hong and A. J. Hopfinger, 3D-pharmacophores of flavonoid binding at the benzodiazepine GABA(A) receptor site using 4D-QSAR analysis, *J. Chem. Inf. Comp. Sci.* **2003**, 43, 324–336.
- [25] A. Hirashima, T. Eiraku, E. Kuwano, E. Taniguchi, and M. Eto, Three-dimensional Pharmacophore Hypotheses of Octopamine Receptor Responsible for the Inhibition of Sex-pheromone Production in *Plodia interpunctella*, *Internet Electron. J. Mol. Des.* **2002**, 1, 37–51, <http://www.biochempress.com>.

Biographies

Akinori Hirashima, Ph.D. is associate professor of pesticide chemistry at Kyushu University at Fukuoka, Japan. Dr. Hirashima formulated the investigation into the structural design of octopamine agonists. After obtaining a Ph.D. degree in synthesis and stereochemistry of organophosphorus insecticides from the Kyushu University in Fukuoka, Dr. Hirashima undertook postdoctoral research with Professor John E. Casida at the Environmental Chemistry and Toxicology Laboratory at the University of California at Berkeley. More recently, Dr. Hirashima has collaborated on projects with Professor Hans-J. Riebel of Chemistry Department at the Bayer AG.

Eiichi Kuwano, Ph.D. is professor of pesticide chemistry at Kyushu University at Fukuoka, Japan. Dr. Kuwano formulated the investigation into the structural design of juvenile-hormone agonists. After obtaining a Ph.D. degree in synthesis of *s*-triazine derivatives from amino acids and peptides and their biological activities from the Kyushu University in Fukuoka, Dr. Kuwano undertook postdoctoral research with Professor T. Roy Fukuto at the Department of Entomology at the University of California at Riverside. More recently, Dr. Kuwano has collaborated on projects with Professor Bruce D. Hammock of the Department of Entomology at the University of California at Davis.

Morifusa Eto, Ph.D. is professor emeritus of pesticide chemistry at Kyushu University at Fukuoka, Japan. Dr. Eto investigated into the structural design of organophosphorus insecticides. After obtaining a Ph.D. degree in cyclic phosphorus esters with toxicity from the Kyushu University in Fukuoka, Dr. Eto undertook postdoctoral research with Professor John E. Casida at the Department of Entomology at the University of Wisconsin at Madison.